Available online at www.sciencedirect.com
ScienceDirect
Journal of Molecular Catalysis A: Chemical 272 (2007) 198–206
JOURNAL OF MOLECULAR CATALYSIS A: CHEMICAL
www.elsevier.com/locate/molcata

Pore size independent regioselective cyclohexylation of ethylbenzene

R. Anuradha, M. Palanichamy, V. Murugesan *

Department of Chemistry, Anna University, Chennai 600025, India

Received 10 February 2007; received in revised form 17 March 2007; accepted 20 March 2007
Available online 24 March 2007

Abstract

Al-MCM-41 (Si/Al = 52 and 105) and Al-MCM-48 (Si/Al = 47 and 102) molecular sieves were synthesised by hydrothermal method. These materials and commercial HY zeolite were characterised by XRD, BET, ^{27}Al MAS-NMR, pyridine adsorbed FT-IR and ICP-AES techniques. The vapour phase cyclohexylation of ethylbenzene (EB) with cyclohexene was carried out between 200 and 400 °C over all the catalysts. The major products were found to be *p*-cyclohexyl ethylbenzene (*p*-CEB) and *o*-cyclohexyl ethylbenzene (*o*-CEB). The activity of the catalysts followed the order Al-MCM-41 (52) > Al-MCM-41 (105) > Al-MCM-48 (47) > Al-MCM-48 (102) > HY. Al-MCM-41 and Al-MCM-48 are more active than HY although the density of acid sites of the former catalysts is less than the latter. This is due to the large pore size of Al-MCM-41 and Al-MCM-48 catalysts that permits simultaneous entry of more reactants into the pores and expulsion of products freely out of the pores. Al-MCM-41 catalysts are more active than Al-MCM-48 catalysts due to more density of acid sites on the channel surface of Al-MCM-41. The selectivity of *p*-CEB is higher than *o*-CEB due to less steric hindrance for its formation. The effects of feed ratio and WHSV on ethylbenzene conversion and product selectivities were evaluated in the above reaction.

Keywords: Zeolite; Al-MCM-41; Al-MCM-48; Cyclohexene; Ethylbenzene

1. Introduction

Alkylation of aromatic hydrocarbons is commercially important and hence it has been studied extensively over solid acid catalysts. Ethylbenzene (EB), propylbenzene, isopropyltoluene and C_{10}–C_{14} linear alkylbenzenes are some of the chemical intermediates obtained by acid catalysed alkylation of aromatics [1,2]. Alkylation of EB, toluene, phenol, etc., are a few of the reactions that have been studied extensively in our lab [3–5]. Alkylation of EB is a reaction of interest as the products on dehydrogenation yield *o*- or *p*-alkylated vinyl benzenes which find applications in the production of alkylated polystyrene with adjustable T_g values. Appropriate alcohols and esters are the commonly employed alkylating agents in all the processes. Zeolites, zeotype molecular sieves and mesoporous Al-MCM-41 molecular sieves have been employed as catalysts in the alkylation reaction. As a continuation of our previous work in this topic, the present study focussed the vapour phase cyclohexylation of EB. This reaction is industrially important as the cyclohexylated ethylbenzene on selective dehydrogenation yields cyclohexyl styrene, which can be polymerized to cyclohexylated polystyrene that possess low T_g values and melting temperatures. They find application as a fixative for ink jet printing [6]. They are also added to rubber composition as additives to improve abrasion resistance and gripping performance. In addition they also improve resistance to bleeding of the components from rubber matrix [7]. The cyclohexylated monomers are also used in the formulation of pressure sensitive adhesives [8,9]. In addition, the cyclohexylated EB can be dehydrogenated to vinyl biphenyl, an important monomer for polypara-vinyl biphenyl derivative [10,11].

Cyclohexylation of EB over solid acid catalysts has not been reported so far in the literature. Hence we are reporting cyclohexylation of EB in the vapour phase over HY, Al-MCM-41 and Al-MCM-48 molecular sieves in this study. Since the zeolite is of large pore type and other materials are mesoporous, they are not expected to impose any constrain for regioselective electrophilic reaction of the reagents in the pores. The *ortho* and *para* substitutions in ethylbenzene are predominant and the *meta* substitution is not activated. Since cyclohexene can be

* Corresponding author. Tel.: +91 44 22203144; fax: +91 44 22200660.
E-mail address: v_murugu@hotmail.com (V. Murugesan).

1381-1169/$ – see front matter © 2007 Elsevier B.V. All rights reserved.
doi:10.1016/j.molcata.2007.03.048

activated by the Brönsted acid sites of the solid acid catalysts, electrophilic cyclohexylation of ethylbenzene may be a feasible one.

2. Experimental

2.1. Preparation of catalysts

The HY zeolite was purchased from Sud-Chemie India Ltd. and used in this study. Hydrothermal crystallisation procedure [12] was adopted for the preparation of Al-MCM-41 molecular sieves with Si/Al ratios 52 and 105 using gel composition of SiO_2:0.2 CTAB:x Al_2O_3:0.89 H_2SO_4:120 H_2O (x varies with Si/Al ratio). In a typical synthesis, sodium metasilicate nona hydrate (Merck) (21.21 g) in water (85 ml) was combined with an appropriate amount of aluminium sulphate (Merck) in distilled water. The pH of the solution was adjusted to 10.5 using 1 M sulphuric acid and stirred continuously to form a gel. After the gel was stirred for 30 min, an aqueous solution of cetyltrimethylammonium bromide (Merck) (7.218 g in 23 ml water) was added and the surfactant-silicate mixture was stirred another 30 min at room temperature. The suspension was then transferred to a stainless steel autoclave, sealed and heated in a hot air oven at 145 °C for about 48 h. The crystallised materials were filtered, washed with distilled water and dried in air at 100 °C. The dried materials were calcined at 550 °C in air for 5 h in a muffle furnace to expel the template.

Al-MCM-48 materials were prepared by the method reported already [13]. Tetraethylorthosilicate (TEOS, Merck), aluminium hydroxide (Merck) and *N*-hexadecyltrimethylammonium bromide (Merck) were the sources for silicon, aluminium and structure directing template, respectively. In a typical synthesis of sodium form of Al-MCM-48, TEOS was slowly added to a solution of *N*-hexadecyltrimethylammonium bromide dissolved in distilled water. Sodium hydroxide solution (1 M) was added to form the gel and maintain the pH as 11.6. The gel was stirred for 30 min at room temperature. Appropriate amount of aluminium hydroxide in 31.2 ml water was stirred separately for 2 h at 80 °C and added to the stirred gel. The resulting mixture was again stirred for 1 h at room temperature, transferred into a polypropylene bottle and kept in an air oven at 100 °C for 72 h for crystallisation. The solid product obtained was filtered, washed and dried at 100 °C. The as-synthesised material was calcined at 550 °C for 1 h in nitrogen atmosphere followed by 6 h in air to remove the template. The H form of Al-MCM-48 was obtained by ion exchange with 1 M ammonium nitrate solution followed by calcination at 550 °C for 6 h in air. The same ion exchange procedure was also applied to Al-MCM-41 catalysts.

2.2. Characterisation of the catalysts

The powder X-ray diffraction patterns were recorded on a PANalytical X'pert PRO diffractometer using Cu Kα radiation ($\lambda = 0.154$ nm) and a liquid nitrogen-cooled germanium solid-state detector. The diffractograms were recorded in 2θ range 5–80° in steps of 0.01° with a count time of 10 s at each point for zeolites, and 2θ range 0.8–10° in steps of 0.02° with a count time of 10 s at each point for Al-MCM-41 and Al-MCM-48. Chemical analysis was performed with ICP-AES Labtum plasma 8440 instrument. The silica content was determined after dissolution of the sample in HF and the alumina content after dissolution in borax.

The surface area and pore properties were measured by nitrogen physisorption at −196 °C with an ASAP-2010 volumetric adsorption analyser (Micrometrics Corporation, Norcross, GA, USA). Before nitrogen adsorption–desorption measurements, the samples were degassed at 350 °C under 10^{-5} mbar overnight. The specific surface area of the samples were determined from the linear portion of BET plots. The pore size distribution was calculated from the desorption branch of nitrogen adsorption–desorption isotherms using the Barett–Joyner–Halenda (BJH) algorithm (ASAP 2010 built-in-software). ^{27}Al MAS-NMR spectra were recorded on a Bruker MSL 400 spectrometer equipped with a magic angle-spinning (MAS) unit. The spectra were recorded at a frequency of 104.22 MHz, a spinning rate of 8 kHz, a pulse length of 1.0 μs, a delay time of 0.2 s and a spectral width of 330 ppm. The total scans were 150 and the line broadening was 50 Hz. ^{27}Al MAS-NMR chemical shifts were reported in relation to the liquid solution of aluminium nitrate.

The acidity of the catalysts was measured using a (Nicolet Avatar 360) FT-IR spectrophotometer equipped with a high temperature vacuum chamber using pyridine as a probe. The sample (approximately 30 mg for HY zeolite and 10 mg for Al-MCM-41 and Al-MCM-48 materials) was taken in the sample holder and dehydrated at 400 °C for 6 h under vacuum (10^{-5} mbar). The sample was then cooled to room temperature and the spectrum was recorded. Then pyridine was adsorbed at room temperature. The physically adsorbed pyridine was removed by heating the sample at 150 °C under vacuum (10^{-5} mbar) for 30 min, the removed material was cooled to room temperature and then the spectrum was again recorded. The acidity was calculated using the extinction coefficient of the bands of Brönsted and Lewis acid sites adsorbed pyridine [14].

2.3. Catalytic reactor set up and product analysis

A mixture of cyclohexene and ethylbenzene was fed into a fixed bed, vertical flow-type reactor, packed with appropriate amount (1 g of HY zeolite or 0.5 g of Al-MCM-41 or Al-MCM-48) of the catalyst. The liquid products collected for 1 h were analysed, after discarding the products collected in the first 10 min. This reaction was carried out at atmospheric pressure. After each catalytic run, the reactor was heated to approximately 500 °C continuously for 6 h by passing moisture and carbon dioxide-free air through it in order to eliminate the deposited coke. The percentage conversion of ethylbenzene was analysed using a gas chromatograph (Shimadzu GC-17A) equipped with a FID detector and a 25 m capillary column (cross-linked 5% phenyl methyl polysiloxane). The products were identified using a gas chromatograph coupled with mass spectrometer

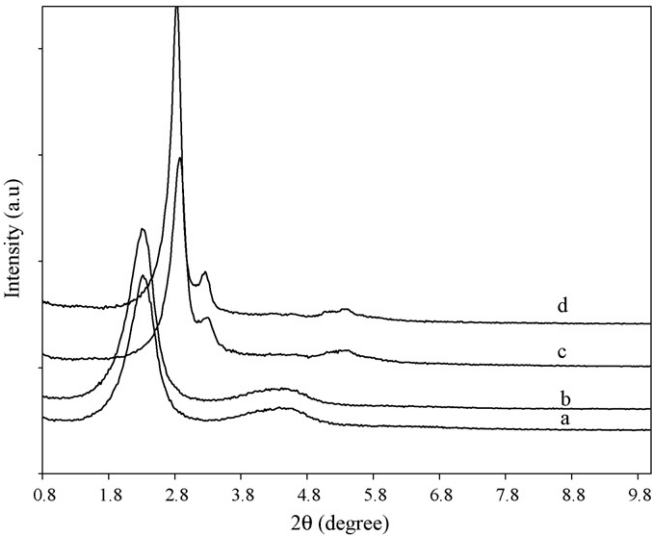

Fig. 1. XRD patterns of (a) Al-MCM-41 (52), (b) Al-MCM-41 (105), (c) Al-MCM-48 (47) and (d) Al-MCM-48 (102).

(Perkin-Elmer Auto System XL) with helium as the carrier gas (1 ml/h).

3. Results and discussion

3.1. Characterisation of the catalysts

3.1.1. XRD

Fig. 1a and b depict the XRD patterns of calcined Al-MCM-41 samples containing Si/Al molar ratios 52 and 105. The patterns resemble similar features as those already reported in the literature for Al-MCM-41 materials [15,16]. The XRD patterns of calcined Al-MCM-41 exhibited an intense peak around 2.3° (2θ) due to (1 0 0) plane and unresolved weak signal of higher order reflections (1 1 0) and (2 0 0) around 3.8° to 5.0° (2θ) indicating the existence of hexagonal phase with $d_{100} = 37.8$ and 38.7 Å for Si/Al ratios 52 and 105, respectively [15]. The unit cell parameter (a_0) was calculated using the formula $2d_{100}/\sqrt{3}$. The d-spacing and a_0 values (Table 1) increase with increase in Si/Al ratio due to decrease in the metal content [17]. After calcination the intense peak shifted to higher 2θ value due to pore size contraction.

The XRD patterns of calcined Al-MCM-48 materials are shown in Fig. 1c and d. It is observed that the calcined samples exhibited an intense peak around 2.8° (2θ) due to (2 1 1) plane reflection, a small peak of higher order reflection (2 2 0) around 3.3° (2θ) and unresolved signal due to (3 2 1), (4 0 0), (4 2 0), (3 3 2), (4 2 2) and (4 3 1) reflections around 5.0° to 5.6° (2θ) indicating the formation of cubic mesophase. The XRD patterns are in good agreement with previous reports for similar materials [18]. The values of cubic unit cell constant ($a_0 = d_{hkl}\sqrt{h^2 + k^2 + l^2}$) and d-spacing values for calcined Al-MCM-48 are given in Table 1. The d-spacings are compatible with cubic $Ia3d$ space group as reported in the literature [12]. It is observed that the unit cell parameter of calcined Al-MCM-41 and Al-MCM-48 samples decreases with decrease in Si/Al ratios. Similar observation was also reported by Krithiga et al. [13] and Romero et al. [19].

3.1.2. Nitrogen adsorption studies

The textural properties (BJH method) of calcined Al-MCM-41 were determined using nitrogen sorption studies and the results are presented in Table 1. The nitrogen adsorption isotherms of calcined materials were measured at liquid nitrogen temperature (−196 °C). The values in Table 1 indicate that pore diameter of Al-MCM-41 materials decreases with increasing Al content due to the presence of textural mesoporosity. The decrease is attributed to framework leaching of Al^{3+} to form non-framework nanoislands of Al_2O_3 in the mesopores [20]. The specific surface area calculated using BET model for all the samples is high, thus exhibiting their mesoporous nature [21]. The specific surface area, specific pore volume and pore diameter of Al-MCM-48 decrease with increase of Al content. This is mainly due to the presence of metal oxide species inside the mesoporous channels of Al-MCM-48 with high Al content. Such observation has been reported in earlier studies for metal substituted cubic and hexagonal type mesoporous materials [22,23].

3.1.3. ^{27}Al MAS-NMR

^{27}Al MAS-NMR spectra of Al-MCM-41 samples are shown in Fig. 2a and b. The peak at 53 ppm is attributed to the presence of aluminium in tetrahedral coordination [20,21]. The calcined materials show a less intense peak around 0 ppm in addition to the peak at 53 ppm. The former peak is due to the non-framework aluminium in octahedral co-ordination. This arises out of the framework de-alumination during calcination, which occurs mainly due to the small amount of tetrahedral aluminium sites bound to the template or water molecule, or due to both [24]. The intensity of peak appeared around 0 ppm decreases with increase in Si/Al ratio [17,25]. Aluminium leaching is commonly observed in Al-MCM-41 with low Si/Al ratios. Since the materials prepared in this study are not of high structural

Table 1
Physico-chemical characteristics of the catalysts

Catalyst	Si/Al	ICP	d_{100} for Al-MCM-41 and d_{211} for Al-MCM-48 (Å)	a_0 (Å)	BET surface area (m^2/g)	Pore volume (cm^3/g)	Pore diameter (Å)	Wall thickness (Å)
Al-MCM-41 (52)	50	52	37.8	43.6	1044	0.75	28.7	14.9
Al-MCM-41 (105)	100	105	38.7	44.7	909	0.69	30.2	14.5
HY (3)	3	–	–	–	648	0.29	7.4	–
Al-MCM-48 (47)	50	47	30.6	75.1	1275	0.52	20.2	14.2
Al-MCM-48 (102)	100	102	31.1	76.1	1350	0.59	21.7	14.4

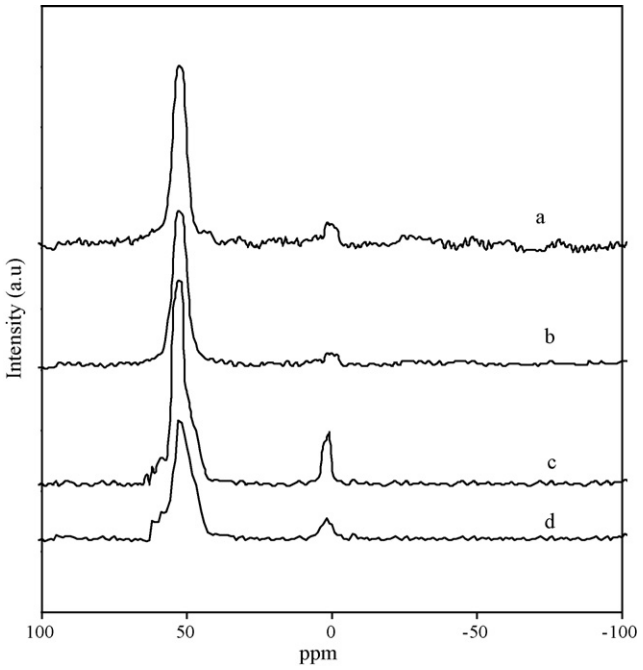

Fig. 2. ^{27}Al MAS-NMR spectra of (a) Al-MCM-41 (52), (b) Al-MCM-41 (105), (c) Al-MCM-48 (47) and (d) Al-MCM-48 (102).

order, Al leaching is observed for Al-MCM-41 even with Si/Al ratio 105. The ^{27}Al MAS-NMR spectra of calcined Al-MCM-48 materials are shown in Fig. 2c and d. The samples exhibit an intense peak at 53 ppm which corresponds to the tetrahedral coordination of Al in the framework. A weak signal around 0 ppm shows the presence of Al in octahedral coordination, which indicates that during calcination some Al species were removed from the framework [26]. The intensity of these peaks increases as the Al content increases. The slight peak broadening of Al signals in the spectra of calcined samples is attributed to highly distorted environment [24,27].

3.1.4. Pyridine adsorbed FTIR spectroscopy

Pyridine adsorbed FTIR spectra of Al-MCM-41 catalysts are shown in Fig. 3a and b. The sharp peak observed around 1545 cm^{-1} for all the catalysts is the typical of adsorption of pyridine over Brönsted acid sites. A less intense peak around 1450 cm^{-1} and a more intense peak around 1620 cm^{-1} are due to pyridine adsorbed on Lewis acid sites. A broad peak around 1490 cm^{-1} is the combination band of Brönsted and Lewis acid sites. These are similar to the spectral data already reported in the literature [28]. The pyridine adsorbed FT-IR spectra of Al-MCM-48 (Si/Al = 47 and 102) are presented in Fig. 3c and d. The peaks at 1613 and 1440 cm^{-1} indicate the presence of Lewis acid sites. The peak at 1490 cm^{-1} is the combination of Lewis and Brönsted acid sites. The peak at 1548 cm^{-1} corresponds to Brönsted acid sites. The more intense peak at 1548 cm^{-1} indicates that the majority of acid sites present in the catalyst are of Brönsted type. The peak intensities of both Brönsted and Lewis acid sites are high for Al-MCM-48 (47) than Al-MCM-48 (102) because of the increased Al content in Al-MCM-48 (47) [28]. The DRIFT spectra of pyridine adsorbed HY zeolite is presented in Fig. 3e. The DRIFT spectra of chemisorbed pyridine reveal that zeolites contain both Brönsted and Lewis acid sites. The existence of Brönsted acid sites in the samples is clearly shown by the bands at 1540 and 1632 cm^{-1} due to ring vibration of pyridine bound to Brönsted acid sites. The bands at 1445 and 1620 cm^{-1} are assigned to pyridine associated with Lewis acid sites. The band at 1490 cm^{-1} is attributed to pyridine chemisorbed on both Brönsted and Lewis acid sites. The band at 1400 cm^{-1} is attributed to pyridine hydrogen bonded to defective Si-OH groups. These acid sites are responsible for the catalytic activity of zeolites. These features are similar to those already reported in the literature [29,30].

3.2. Cyclohexylation of ethylbenzene

Cyclohexylation of ethylbenzene with cyclohexene was investigated over HY, Al-MCM-41 (Si/Al = 52 and 105) and Al-MCM-48 (Si/Al = 47 and 102) in the vapour phase. The effects of reaction temperature, feed ratio, WHSV and time-on-stream were studied to optimise the parameters for high ethylbenzene conversion and products selectivity. The major products as analysed by GC-MS were *p*-cyclohexyl ethylbenzene (*p*-CEB), *o*-cyclohexyl ethylbenzene (*o*-CEB), cyclohexylbenzene (CB), dicyclohexane (DC) and dicyclohexyl ethylbenzene (DCEB).

3.2.1. Effect of temperature

The vapour phase cyclohexylation of ethylbenzene (EB) was carried out from 200 to 400 °C over Al-MCM-41 (Si/Al = 52 and 105), Al-MCM-48 (Si/Al = 47 and102) and HY with a feed ratio (EB:cyclohexene) 1:3 and WHSV 3.3 h^{-1}. The results are presented in Tables 2 and 3. EB conversion increases from 200 to 250 °C and then decreases over HY zeolite. The decrease above 250 °C is attributed to coke formation. The pathway for the formation of different products is depicted in Scheme 1. The following explanation will account for the formation of different products. Cyclohexene chemisorbed on the Brönsted

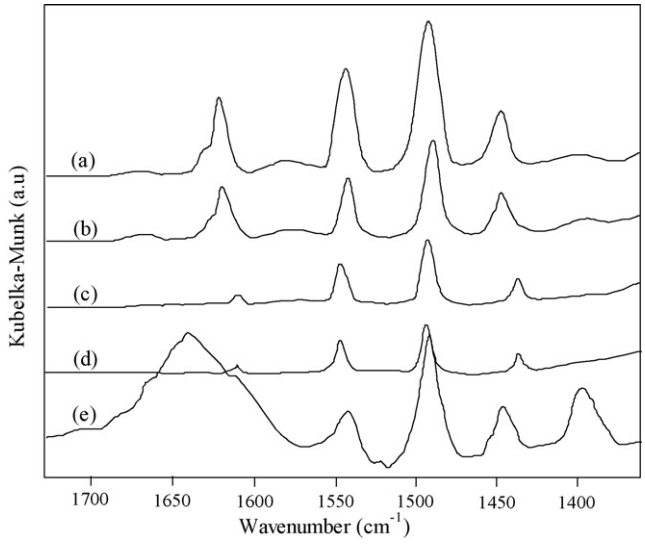

Fig. 3. Pyridine adsorbed FTIR spectra of (a) Al-MCM-41 (52), (b) Al-MCM-41 (105), (c) Al-MCM-48 (47), (d) Al-MCM-48 (102) and (e) HY.

Table 2
Conversion and products selectivity over HY and Al-MCM-41 catalysts at various temperatures

Catalyst	Temperature (°C)	Conversion of EB (%)	Products selectivity (%)					
			o-CEB	*p*-CEB	DCEB	CB	DC	Others
HY	200	44	26	59	0	6	7	2
	225	47	23	60	0	7	7	3
	250	49	19	61	0	8	9	3
	275	40	16	62	0	8	10	4
	300	38	13	63	0	9	10	5
	350	31	10	63	0	10	11	6
	400	25	5	65	0	11	12	7
Al-MCM-41 (52)	200	79	25	53	0	9	9	4
	225	81	21	54	0	10	10	5
	250	82	20	55	0	10	10	5
	275	73	16	56	0	11	11	6
	300	69	13	57	2	11	11	6
	350	65	8	59	3	12	12	6
	400	57	4	60	3	13	13	7
Al-MCM-41 (105)	200	71	28	47	0	10	10	5
	225	75	26	48	0	11	10	5
	250	79	22	49	0	12	11	6
	275	70	18	50	0	13	12	7
	300	61	13	52	1	13	13	8
	350	58	9	53	3	14	13	8
	400	43	4	53	4	16	14	9

Reaction conditions: weight of the catalyst = 0.5 g; feed ratio = 1:3 (EB:cyclohexene); time on stream = 1 h; WHSV = 3.30 h^{-1}. *Note*: CB = cyclohexylbenzene, DC = dicyclohexane, *p*-CEB = *para*-cyclohexyl ethylbenzene, *o*-CEB = *ortho*-cyclohexyl ethylbenzene, DCEB = dicyclohexyl ethylbenzene.

acid sites of the catalyst yielding cyclohexyl cation takes part in the electrophilic reaction with ethylbenzene either in the vapour phase or closely chemisorbed cyclohexene on the Brönsted acid sites, thus yielding *o*-CEB and *p*-CEB (Scheme 1). Cyclohexyl cation can also react electrophilically with another cyclohexene molecule yielding dicyclohexyl cation, which in turn gives dicyclohexane by accepting a hydride ion or dicyclohexene (included as others) with the elimination of a H^+ ion. The dehydrogenation of cyclohexene to benzene is the source reaction to account for the hydride ion. The cracking of ethylbenzene on the active sites produces benzene, which reacts with cyclohexyl cation yielding CB (Scheme 1).

The selectivity to *o*-CEB decreases with increase in temperature whereas *p*-CEB increases with increase in temperature. The selectivity to *p*-CEB is higher than *o*-CEB as its formation is free of steric hindrance. Though the formation of *o*-CEB is sterically hindered, the decrease in selectivity with increase in temperature is attributed to rotation of ethyl group with respect to the plane of benzene ring. Based on the values of selectivity it could be visualised that the rotation might be higher at higher

Table 3
Conversion and products distribution of cyclohexylation of ethylbenzene over Al-MCM-48 catalysts at various temperatures

Catalyst	Temperature (°C)	Conversion of EB (%)	Products selectivity (%)					
			o-CEB	*p*-CEB	DCEB	CB	DC	Others
Al-MCM-48 (47)	200	51	30	43	0	9	12	6
	225	56	26	44	0	11	13	6
	250	59	23	45	0	12	14	6
	275	50	19	46	0	12	16	7
	300	46	14	47	1	13	17	8
	350	39	12	47	2	14	17	8
	400	34	7	48	3	14	18	10
Al-MCM-48 (102)	200	48	30	42	0	9	13	6
	225	51	27	43	0	10	13	7
	250	55	23	44	0	11	14	8
	275	46	19	46	0	11	16	8
	300	40	15	47	1	13	16	8
	350	36	11	47	1	14	18	9
	400	32	5	48	2	15	19	11

Reaction conditions: weight of the catalyst = 0.5 g; feed ratio = 1:3 (EB:cyclohexene); time on stream = 1 h; WHSV = 3.30 h^{-1}. *Note*: CB = cyclohexylbenzene, DC = dicyclohexane, *p*-CEB = *para*-cyclohexyl ethylbenzene, *o*-CEB = *ortho*-cyclohexyl ethylbenzene, DCEB = dicyclohexyl ethylbenzene.

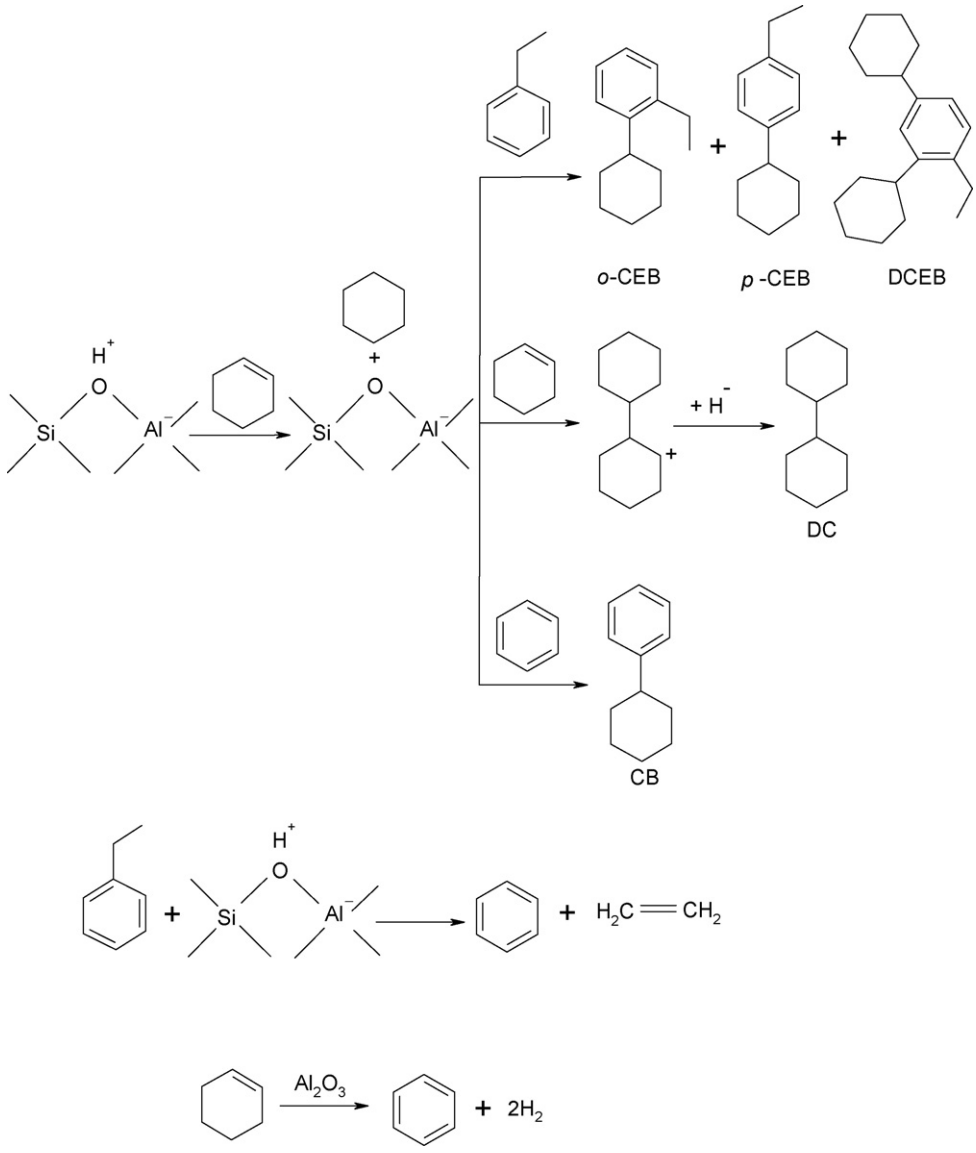

Scheme 1. Reaction of ethylbenzene with cyclohexene.

temperature. Since the rotation at higher temperature drastically reduces electrophilic reaction at both *o*-positions, the selectivity to *p*-CEB increases. It could be presumed that free rotation of ethyl group can induce electrophilic reaction even at m-position as free rotation suppresses activating influence of ethyl grouping. But this product was not observed over any of the catalysts used in this study. The σ complex formed as a result of electrophilic attack at *o*- and *p*-positions are therefore expected to be stabilised by resonance interaction with ethyl group, but it requires suppression of free rotation of ethyl group. One could easily understand this fact as the σ complex produces positive charge on the carbon bearing ethyl group by which resonance can be enhanced by suppressing rotation. Such free rotation has already been reported in the literature [31]. As mentioned above the increase in selectivity to *p*-CEB is due to extra availability of cyclohexyl cation for electrophilic reaction at the para position as a result of suppression of the same at *o*-position.

Although *o*-CEB and *p*-CEB were observed, DCEB was present as its formation is more activation energy demanding than *o*-CEB or *p*-CEB. Such high activation energy demand for consecutive alkylation has been reported in the literature [32]. As a result DCEB was not observed at lower temperatures over HY and mesoporous catalysts. It was not observed over HY even at higher temperatures. Since coke formation predominates inside the zeolite pore at higher temperatures, it is expected to offer significant constrain for the formation of large space demanding DCEB. The effect of pore size contraction due to coke formation for the selective formation of *p*-CEB is best realised in this study. The formation of CB reveals cracking of EB to benzene and subsequent cyclohexylation. The cracking of EB was established by passing EB as such over the catalyst. In addition, the minor products given in the last column of Tables 2 and 3 also include benzene. The selectivity to CB increases with increase in temperature due to increase of benzene

content and decrease of cyclohexyl cation content. The gradual increase in the rate of reaction between cyclohexyl cation and EB may be the cause for decrease of cyclohexyl cation. High selectivity of DC demands more free cyclohexene whose content could increase with increase in temperature.

The conversion of EB over Al-MCM-41 (52) was higher than over HY zeolite. This is due to easy entry of reactants into the large pores and expulsion of products out of the pores. Similar to HY zeolite, the conversion also increases upto 250 °C and then decreases over Al-MCM-41 (52) and the decrease is due to coke formation. The selectivity to *o*-CEB, *p*-CEB, CB and DC exhibits the same trend as over HY zeolite. The selectivity to DCEB appears different and this product is not observed upto 275 °C. But above 275 °C, selectivity of DCEB is less than 4% at all temperatures. Unlike HY zeolite, Al-MCM-41 does not suffer much pore size reduction and hence the constraint for the formation of DCEB will not exist and this is clearly reflected in its selectivity. The selectivity to CB and DC exhibits the similar trend as that of HY zeolite.

The conversion and products selectivity over Al-MCM-41 (105) show similar trend as that of Al-MCM-41 (52). Although the density of acid sites of this catalyst is nearly 50% less than that of Al-MCM-41 (52) but the activity is close to that of Al-MCM-41 (52) which illustrates the importance of the strength of Brönsted acid sites. Since Si/Al ratio in Al-MCM-41 (105) is higher than Al-MCM-41 (52), the enhanced acid strength might compensate the less density of acid sites in order to give such high conversion [33].

The conversion and products selectivity over Al-MCM-48 (47) and Al-MCM-48 (102) also show similar behaviour as that of Al-MCM-41. Unexpectedly the conversion over both these catalysts is less than Al-MCM-41 catalysts. These catalysts possess nearly similar Si/Al ratios as that of Al-MCM-41 catalysts, still the conversion is less. The high surface area of these catalysts is also not conforming to the activity results as their surface area are higher than Al-MCM-41 catalysts. Acidity measurements, as illustrated in Fig. 3, show less Brönsted acidity than Al-MCM-41 catalysts, which suggest planting of aluminium in the bulk portion of the mesoporous wall rather than on the channel surface. Though Al-MCM-48 (102) possesses less density of Brönsted acidity, it shows nearly same conversion as that of Al-MCM-48 (47). Hence the enhancement of acid strength due to high Si/Al ratio might play an important role in enhancing conversion similar to that of Al-MCM-41. This discussion reveals that Al-MCM-41 (52) is the most active catalyst at an optimum temperature of 250 °C.

3.2.2. Effect of feed ratio

The effect of feed ratio on conversion and product selectivity was studied over Al-MCM-41 (52) at 250 °C with WHSV 3.3 h^{-1}. The results are depicted in Fig. 4. The conversion increases from feed ratio 1:1 to 1:3 but decreases at 1:5. This suggests that chemisorption of cyclohexene may be increased from 1:1 to 1:3 which enhances the conversion. The decrease of conversion at 1:5 is the cause of dilution of EB by excess cyclohexene, which reduce the electrophilic reaction with cyclohexyl cation. The selectivity to *o*-CEB and *p*-CEB increases from 1:1 to 1:3 but decreases at 1:5. This observation clearly supports dilution of EB by excess cyclohexene at 1:5 feed ratio. It is also supported by increase in the selectivity of DC. The selectivity to CB also illustrates dilution of EB by cyclohexene at 1:5 whose selectivity gradually decreases from 1:1 to 1:5. The cracking of EB to benzene is reduced due to dilution, which is actually the precursor of CB. In order to verify this, the reaction was also studied at feed ratios 2:1 and 3:1. In line with our view the selectivity of CB increased from 2:1 to 3:1. The conversion of EB and the selectivity to *o*-CEB and *p*-CEB also decrease in the same order. This study clearly illustrates the competitive adsorption of EB on the active sites of catalyst. The optimum feed ratio is found to be 1:3.

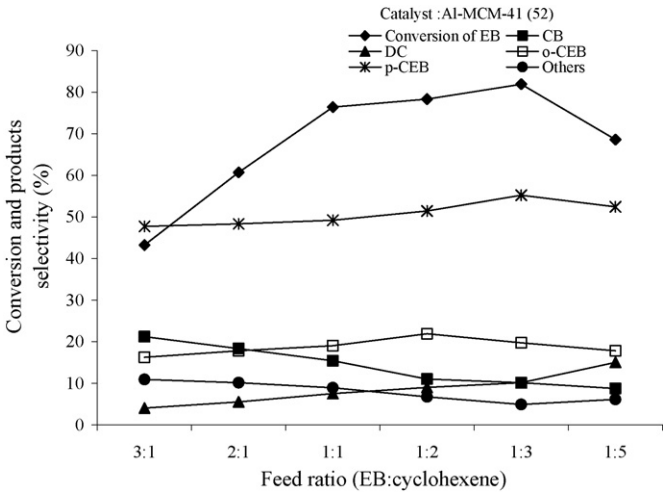

Fig. 4. Effect of feed ratio on conversion and products selectivity. Reaction conditions: temperature = 250 °C; WHSV ~3.3 h^{-1}; time on stream = 1 h.

3.2.3. Effect of WHSV

The effect of WHSV was studied over Al-MCM-41 (52) at 250 °C with the feed ratio 1:3 and the results are shown in Fig. 5.

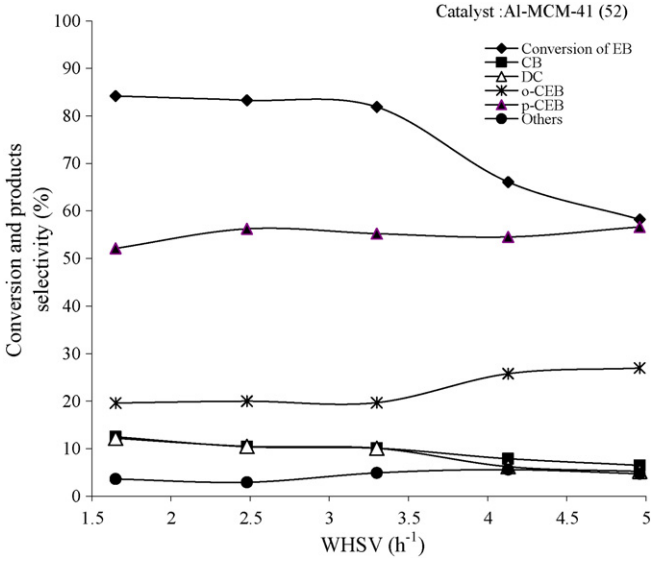

Fig. 5. Effect of WHSV on conversion and products selectivity. Reaction conditions: temperature = 250 °C; feed ratio = 1:3 (EB:cyclohexene); time on stream = 1 h.

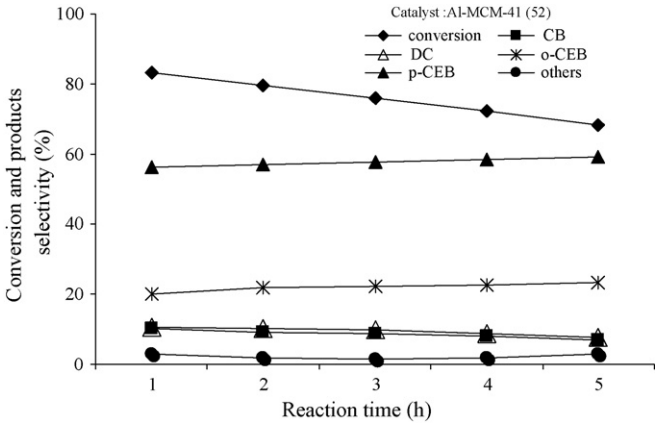

Fig. 6. Effect of time on stream on conversion and products selectivity. Reaction conditions: temperature = 250 °C; feed ratio = 1:3 (EB:Cyclohexene); WHSV = 2.48 h^{-1}.

As expected the conversion decreases with increase in WHSV. There is a sudden fall in conversion above 3.3 h^{-1}. This illustrates the rapid rate of diffusion of reactants with suppressed chemisorption above 3.3 h^{-1}. The selectivity to *o*-CEB shows nearly similar values upto 3.3 h^{-1} but between 3.3 and 4.13 h^{-1}, there is a sudden increase in the selectivity due to less cracking of EB and dehydrogenation of cyclohexene. The sudden drop in the selectivity of CB and DC between 3.3 and 4.13 h^{-1} also supports this. The selectivity of *p*-CEB is higher than all other products at all WHSVs. Based on conversion and selectivity to *p*-CEB, WHSV of 2.48 h^{-1} is found to be the optimum one.

3.2.4. Effect of time on stream

The sustainability of Al-MCM-41 (52) was evaluated by conducting the time on stream study for 5 h at 250 °C with a feed ratio of 1:3 (ethylbenzene:cyclohexene) and WHSV (2.48 h^{-1}). The plot of conversion and product selectivity versus time is illustrated in Fig. 6. The conversion decreases gradually with the increase in time on stream because of gradual increase in blocking of active sites by coke. The selectivity to *o*-CEB and *p*-CEB increases but the increase is not significant. The small increase is due to the consequent decrease in the selectivity of CB and DC. As coke formation generally predominates over strong acid sites, cracking of EB and dehydrogenation of cyclohexene, the source reaction for CB and DC decrease. The reaction was repeated twice but there is no significant difference in conversion and selectivity.

4. Conclusions

Based on the results, it is concluded that electrophilic reaction occurs on an aromatic substrate at specific position predicted by the inherent electronic factor and steric hindrance and not on the nature of shape-selective catalysts. Although the reaction was not carried over medium pore zeolites like ZSM-5, the deliberate rejection of it is due to the expected less conversion like HY zeolite. Large pore HY zeolite and mesoporous Al-MCM-41 and Al-MCM-48 molecular sieves are therefore suggested to be good choice. When the external selectivity features are not demanded, Al-MCM-41 is more advantageous than HY based on high conversion feasibility. In addition to high conversion, the absence of isomerisation of o-CEB and *p*-CEB to meta-cyclohexyl ethylbenzene is an added advantage. The delayed coke formation due to rapid diffusion is also an additional feature with these mesoporous catalysts.

Acknowledgements

The authors are grateful to Department of Science and Technology (DST) and University Grants Commission (UGC), New Delhi for providing funds under FIST and Special assistance-DRS, respectively, for the excellent instrumental facilities. One of the authors V. Murugesan is thankful to DST, New Delhi for the funds under SERC sponsored project and the author R. Anuradha is thankful to CSIR, New Delhi, for the award of Senior Research Fellowship.

References

[1] H.G. Frank, J.W. Stadehofer, Industrial Aromatic Chemistry, Springer, Berlin, 1998.
[2] C. Perego, P. Ingallina, Catal. Today 73 (2002) 3.
[3] A. Vinu, K. Shanmugapriya, G. Chandrasekar, V. Murugesan, K. Ariga, J. Nanosci. Nanotechnol. 5 (2005) 542.
[4] K. Shanmugapriya, M. Palanichamy, V. Murugesan, Catal. Commun. 7 (2006) 47.
[5] K. Shanmugapriya, R. Anuradha, M. Palanichamy, B. Arabindoo, V. Murugesan, J. Mol. Catal. 221 (2004) 145.
[6] H.-L. Yau, D.S. Uerz, W.S. Krzemien, C.R. Salerno, Application #: 20060004136, Class: 524505000 (USPTO).
[7] K. Nishioka, T. Mabuchi, K. Terakawa, K. Muraoka, Application #: 20060100306, Class: 523160000 (USPTO).
[8] P. Lien, H.J. Patrick, F. Rajeev, European Patent Publication No.: EP0942003.
[9] R. Jovanovicǐ, M.A. Dubeǐ, J. Macromol. Sci. Part C Polym. Rev. C44 (2004) 1.
[10] C. Lourdes, R.J. Antonio, M. Ana, J. Polym. Sci. Part A Polym. Chem. 40 (2002) 3893.
[11] I.A. Katime, T. Nuño, Polym. Bull. 22 (1989) 505.
[12] J.S. Beck, J.C. Vartuli, W.J. Roth, M.E. Lernowicz, C.T. Kresge, K.D. Schmitt, C.T.W. Chu, D.H. Olson, E.W. Sheppard, S.B. McCullen, J.B. Higgins, J.C. Schlenker, J. Am. Chem. Soc. 121 (1992) 10834.
[13] T. Krithiga, A. Vinu, K. Ariga, B. Arabindoo, M. Palanichamy, V. Murugesan, J. Mol. Catal. A: Chem. 237 (2005) 238.
[14] C.A. Emies, J. Catal. 141 (1993) 347.
[15] X.S. Zhao, G.Q. Lu, G.J. Millar, Catal. Lett. 38 (1996) 33.
[16] J.H. Kim, M. Tanabe, M. Niwa, Micropor. Mater. 10 (1997) 85.
[17] R. Mokaya, W. Jones, J. Catal. 172 (1997) 211.
[18] Y. Xia, R. Mokaya, J. Phys. Chem. B 107 (2003) 6954.
[19] A.A. Romero, M.D. Alba, J. Klinowski, J. Phys. Chem. B 102 (1998) 123.
[20] T.R. Pauly, Y. Liu, T.J. Pinnavaia, S.J.L. Billinge, T.P. Rieler, J. Am. Chem. Soc. 121 (1992) 8835.
[21] S. Biz, M.G. White, J. Phys. Chem. B 103 (1999) 8432.
[22] H. Kosslick, G. Lischke, H. Landmessre, B. Partitz, W. Storek, R. Fricke, J. Catal. 176 (1998) 102.
[23] M. Kruk, M. Jaroniec, A. Sayari, Langmuir 15 (1999) 5683.
[24] K. Chaudhari, T.K. Das, A.J. Chandwadkar, S. Sivasanker, J. Catal. 186 (1999) 81.
[25] K. Shanmugapriya, M. Palanichamy, B. Arabindoo, V. Murugesan, J. Catal. 224 (2004) 347.
[26] S.E. Dapurkar, P. Selvam, Appl. Catal. A 254 (2003) 239.

[27] M. Hartmann, C. Bischof, J. Phys. Chem. B 103 (1999) 6230.
[28] A. Corma, V. Fornes, M.T. Navario, J. Perez-Pariente, J. Catal. 148 (1994) 569.
[29] A. Corma, Chem. Rev. 95 (1995) 559.
[30] A. Corma, Micropor. Mesopor. Mater. 4 (1997) 249.
[31] P. Kamalaa, A. Pandurangan, Catal. Lett. 110 (2006) 39.
[32] K. Shanmugapriya, S. Saravanamurugan, M. Palanichamy, B. Arabindoo, V. Murugesan, J. Mol. Catal. A: Chem. 223 (2004) 177.
[33] A. Corma, V. Fornes, M.T. Navarro, J. Perez Pariente, J. Catal. 148 (1994) 569.